PROGRESS IN COLOR, COLORANTS AND COATINGS

available online @ www.pccc.icrc.ac.ir

Progress in Color Colorants Coating 20 (2027), 193-201

Ministry of Science, Research and Technology
Institute for Color Science & Technology

Synthesis of Copper Oxide Nano Powders: Effect of Surface Modifier Type

M. Shafiee Afarani[*1], A. M. Arabi[2], H. Kordi-Tamandani[3], F. Ramezani[3], M. Kaykhaii[4]

[1.] Department of Materials Engineering, Faculty of Engineering, University of Sistan and Baluchestan, P.O. Box: 98135-987, Zahedan, Iran

[2.] Department of Inorganic Pigments and Glazes, Institute for Color Science and Technology, P.O. Box: 16765-654, Tehran, Iran

[3.] Department of Chemistry, Faculty of Science, University of Sistan and Baluchestan, Zahedan, Iran

[4.] Department of Analytical Chemistry, Faculty of Natural Sciences, Comenius University Bratislava, Mlynská Dolina CH-2, Ilkovičova 6, SK-842 15 Bratislava, Slovakia

ARTICLE INFO

Article history:
Received: 02 May 2026
Final Revised: 30 Jun 2026
Accepted: 01 Jul 2026
Available online: 25 Aug 2026

Keywords:
Surface modifiers
Nano-particles
Copper oxide
Precipitation
Band gap

ABSTRACT

CuO nano particles were synthesized via precipitation route in the presence of various surface modifiers (SMs) including Sodium dodecyl sulfate (SDS) and Polyethylene glycol (PEG), (3-Glycidoxypropyl) trimethoxysilane (3-GPTMS), Triton X-100 , Ethylene glycol ($C_2H_6O_2$) and Oleic Acid. The effects of the SMs type on the structure, microstructure and band gap of samples were studied. Results generally showed that the SMs type led to formation of nanostructured monoclinic CuO phase with no considerable change in the structure and with crystallite size of ≤10nm. Furthermore, Fourier transform infrared (FTIR) spectra represented corresponding bands of Cu-O bonds in all samples. Moreover, scanning electron micrographs showed that highly agglomerated semispherical nano particles were obtained. Moreover, transmission electron micrographs showed synthesis in the presence of SDS and 3-GPTMS led to smallest and largest nano particles. Furthermore, considerable band gap broadening of powders up to 4 eV confirms the nano nature of synthesized particles even in quantum region. Prog Color Colorants Coat. 20 (2027), 193-201© Institute for Color Science and Technology.

1. Introduction

Copper oxide (CuO) nanoparticles have been widely interested owing to their outstanding physico-chemical properties arising from their narrow band gap, high surface activity, and strong size-dependent quantum effects. Monoclinic CuO acts as a p-type semiconductor with a bulk band gap of approximately 1.2-1.5 eV, making it suitable for optoelectronic devices [1], gas sensors [2-4], photocatalysis [5-10], antimicrobial coatings, energy conversion [11], and environmental remediation [1, 5]. When CuO is engineered at the nanoscale, its electronic structure, optical absorption, catalytic activity, and surface reactivity can be dramatically modified, enabling applications that are not accessible to the bulk material [12, 13].

Among various synthetic routes, chemical precipitation has emerged as a scalable and practical approach for preparing CuO nano powders with controllable size and morphology. This method relies on the controlled hydrolysis and precipitation of copper salts, typically followed by thermal or chemical conversion to CuO. Its advantages include simplicity,

*Corresponding author: * shafiee@eng.usb.ac.ir
https://doi.org/10.30509/pccc.2026.167790.1501

low cost, mild reaction conditions, and compatibility with large-scale production [1, 13, 14]. However, a persistent challenge in precipitation-based synthesis is the strong tendency of freshly formed CuO nuclei to aggregate and grow uncontrollably, leading to broad size distributions, irregular morphologies, and loss of nanoscale properties [15-17].

To overcome this limitation, surface modifiers such as surfactants, polymers, and organosilanes are widely used as stabilizing and structure-directing agents. These molecules adsorb on the growing nanoparticle surfaces, reduce surface energy, and provide either electrostatic or steric repulsion that suppresses aggregation and allows controlled crystal growth [18]. Anionic surfactants such as sodium dodecyl sulfate (SDS) can induce strong electrostatic stabilization, while non-ionic polymers such as polyethylene glycol (PEG) provide steric hindrance and improve colloidal stability. Organosilanes such as 3-glycidyloxypropyl trimethoxy-silane (3-GPTMS) introduce covalent surface anchoring, improving particle dispersion and functionalizability [14, 18].

The SMs selection can strongly affect the final particle size, crystallinity, morphology, and optical band gap of CuO nanoparticles. For example, PEG-stabilized CuO particles typically show sizes in the 20-30 nm range, while SDS can yield ultra-small particles below 10 nm, approaching the quantum dot regime [5, 14]. Such size reduction leads to a pronounced widening of the band gap due to quantum confinement, with reported values increasing from the bulk ~1.2 eV to above 2.5-3.5 eV for nanometric CuO [12, 18]. This tunability of electronic structure is particularly important for photocatalytic and sensing applications, where band gap engineering directly influences charge transport and light absorption.

Recent studies further demonstrate that CuO nanoparticles synthesized using surfactant-assisted or green precipitation methods exhibit enhanced photocatalytic, antibacterial, antioxidant, and enzyme-inhibitory activities compared with bulk CuO [5, 12, 19]. The improvement is attributed to their reduced size, increased surface area, and higher density of active sites. Moreover, hybrid strategies combining controlled precipitation with stabilizing agents or bio-derived capping molecules provide new routes for producing CuO nanostructures with tailored properties for environmental and biomedical applications [12, 19].

Despite the extensive literature on CuO nanoparticle synthesis [20-23], systematic comparative studies on how different classes of surface modifiers (ionic surfactants, non-ionic polymers, and silane coupling agents) govern particle size, morphology, surface chemistry, and band gap in precipitation-based synthesis are still limited [24-26]. In particular, direct comparisons between electrostatic (e.g., SDS), steric (e.g., PEG), and covalently binding (e.g., 3-GPTMS) stabilizers under identical synthesis conditions remain scarce, even though such information is essential for rational design of CuO nanomaterials for specific applications [14].

In this regard, CuO nano powders were synthesized by a controlled precipitation route using copper acetate as precursor in the presence of different surface modifiers, including SDS, polyethylene glycol (PEG), and 3-GPTMS, as well as non-ionic organic stabilizers. By systematically varying the type of these modifiers, their effects on structure, surface chemistry, morphology, and optical band gap of synthesized powders were investigated. The combined use of XRD, SEM, TEM, and FTIR, UV-Vis spectroscopy techniques, enables a comprehensive understanding of how surface chemistry controls nanoscale growth and electronic structure. This approach provides a unified framework for tailoring CuO nanoparticles from quantum-sized (<10 nm) to larger nanocrystals (20-40 nm) with tunable optical and structural properties, offering valuable insights for advanced applications in catalysis, sensing, and functional nanomaterials.

2. Experimental

Two sets of SMs were considered for experimental tests: first set including Sodium dodecyl sulfate (SDS, $C_{12}H_{25}NaO_4S$, MERCK) and Polyethylene glycol (PEG, $HO(C_2H_4O)_nH$, 400, MERCK), (3-Glycidoxy-propyl) trimethoxysilane (3-GPTMS, $C_9H_{20}O_5Si$, MERCK), and the second set were Triton X-100 ($C_{14}H_{22}O(C_2H_4O)n$, MERCK), Ethylene glycol ($C_2H_6O_2$, MERCK), Oleic Acid ($C_{18}H_{34}O_2$, May & Baker).

Copper oxide powders were synthesized via precipitation route according to procedures reported in some literatures [27-29]. First, 0.3993 g copper acetate monohydrate [$Cu(CH_3COO)_2.H_2O$, Alfa Chemicals] was dissolved in 100 mL distilled water in a beaker to prepare an aqueous solution (0.02M). Then, 0.5 mL acetic acid (CH_3COOH, MERCK) was added to the solution under magnetic agitating at RT for 5 min. After that, addition of SMs was performed as 0.015 g

of SDS/PEG, 0.015 ml of 3-GPTMS, 0.03 mL of EG, 0.06 of Triton-X100, and 0.03 mL of Oleic acid to the resultant solution. Thereafter, 0.5g NaOH (MERCK) was instantly added to the solution under stirring at 70 °C for 10 min. Finally, the black gained precipitates were washed by mixture of acetone and distilled water with ratio of 4:1 and dried in an electric oven at 80 °C for 1h. It should be noted that NaOH agent was selected for getting high pH value in short time intervals. Moreover, experiments were not performed at room temperature to avoid formation of hydrated copper oxide phase. In other words, temperature and pH could control nucleation vs. growth rates in CuO synthesis. Higher pH favors rapid nucleation and smaller particles, while temperature influences dehydration of $Cu(OH)_2$ intermediate [30].

Two Fourier transform infrared spectroscopes (FTIR) were used for molecular studies: i) Bruker TENSOR II which had platinum ATR accessory, and ii) Perkin Elmer Spectrum Two. X-ray diffraction (XRD, Bruker Advance D8) technique was used for structural studies. Two scanning electron microscopes (SEM, KYKY EM3900 and SEM, LEO 1455 VP) and one transmission electron microscope (TEM, Zeiss - EM10C-100kV) were used for microstructure analyses of samples. One UV-Vis spectrophotometer (OPTIZEN 2120UV plus) was used for obtaining UV-visible absorption spectra. Optical Band gaps of synthesized powders were calculated based on the Tauc equation according to [31], by drawing $(\alpha h\nu)^2$ as a function of hν, where h, α and ν are Plank constant, absorption coefficient and frequency (s^{-1}), respectively.

3. Results and Discussions

Figure 1 shows XRD patterns of samples synthesized using various SMs. As illustrated, all samples exhibit dominate phase of monoclinic CuO (Card No. 01-080-1268), with no detectable secondary phases (such as $Cu(OH)_2$ and Cu_2O), indicating high phase purity. In another words, the SMs addition had no effect on the obtained crystalline phase. The broadening of XRD peaks is attributed to formation of nanocrystalline CuO particles due to the SMs addition as particle growth inhibitor. Moreover, the slight difference broadening of the main peak may be related to variation of the chemical nature, charge, and surface coverage of the SMs. In all samples, the two main monoclinic peaks at $2\theta=35.5°$ and 38.7°, corresponding to the (002) and (111) planes, can be observed. However, more desirable crystallization in the presence of EG and oleic acid results in appearance of additional monoclinic peaks at 32.5°, 48.7°, 53.5°, and 58.3°, which respectively correspond to the (110), (-202), (020), and (202) planes. Unlike some SMs such as polyvinylpyrrolidone, which induce a preferred orientation along the (002) planes [32], no preferred orientation is observed in the diffraction patterns.

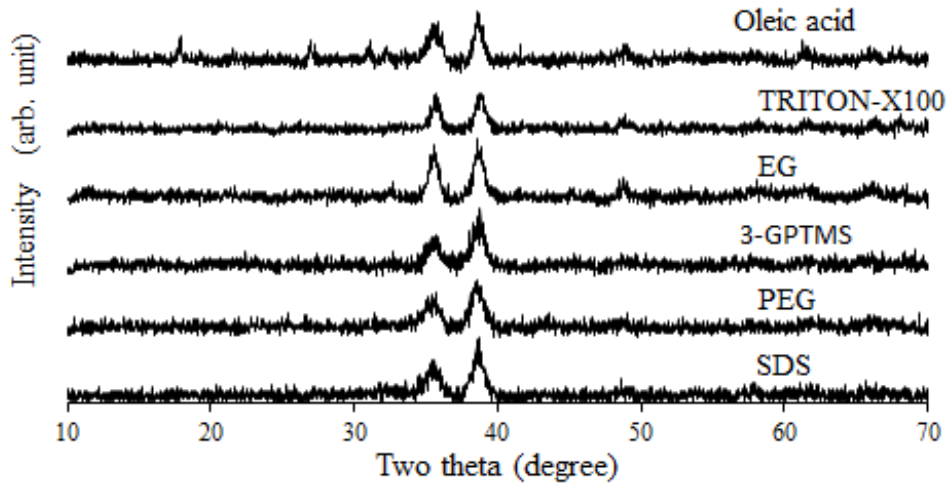

Figure 1: XRD patterns of CuO nano particles synthesized in the presence of various SMs.

Using the Scherrer equation, the mean crystallite size of synthesized powders calculated for the (111) plane are in the range of 6 to 10 nm, confirming a nanocrystalline structure. The crystallite size depends on the type of SMs, with increasing values for SDS, PEG, Triton X-100, 3-GPTMS, EG, and oleic acid being 6, 7, 7, 8, 10, and 10 nm, respectively. This trend reflects the interaction and surface capping effect of the SMs on the particles. The crystallite size variation is due to the different nature of the SMs, their influence on the coverage of primary particles, and differences in steric hindrance and growth control. For instance, comparing PEG and EG, the bulkier PEG prevents crystal growth due to steric repulsion. Although the crystallite size is more than twice that of CuO quantum dots modified with PVP, Tween-80, and CTAB (2-3 nm) mentioned earlier (28), it still remains well below the range observed with SMs such as stearic acid (22 nm) [33].

Figure 2a shows the FTIR spectra of the first set of CuO samples synthesized using PEG, SDS and 3-GPTMS SMs. The main bands at about 415-430 and 588-593 cm^{-1} are related to Cu-O bonds. Figure 2b also illustrates the FTIR spectra of the second set of CuO samples synthesized using EG, Triton-X100 and Oleic acid. In all samples, the peaks below 800 cm^{-1} correspond to metal–oxygen bonds (28, 34). The Cu–O stretching vibrational bands are observed at around 460, 580, and 650 cm^{-1}, confirming the CuO compound formation in all samples [34]. Additionally, the bands in the ranges of 1600 and 3400 cm^{-1} are due to the bending and stretching vibrations of OH groups, respectively, originating from moisture on the surface of CuO particles [35], surface hydroxyl groups, or OH groups from certain SMs such as PEG/EG [32]. Moreover, the bands appearing in the 1300-1600 cm^{-1} range are associated to the bending vibrations of C–H groups and the stretching vibrations of $–CH_2–$ groups due to synthesis in the present of SDS/Oleic acid/Triton 100 [36]. Two bands around 790 and 1000 cm^{-1} are due to Si-O bonds remained from 3-GPTMS [37]. Other bands are related to the other functional groups of SMs. Notably, in Figure 2b, the presence of multiple, strong, and well-defined peaks in the 1000-1700 cm^{-1} range indicates a strong interaction of this group of SMs with the CuO particles' surface.

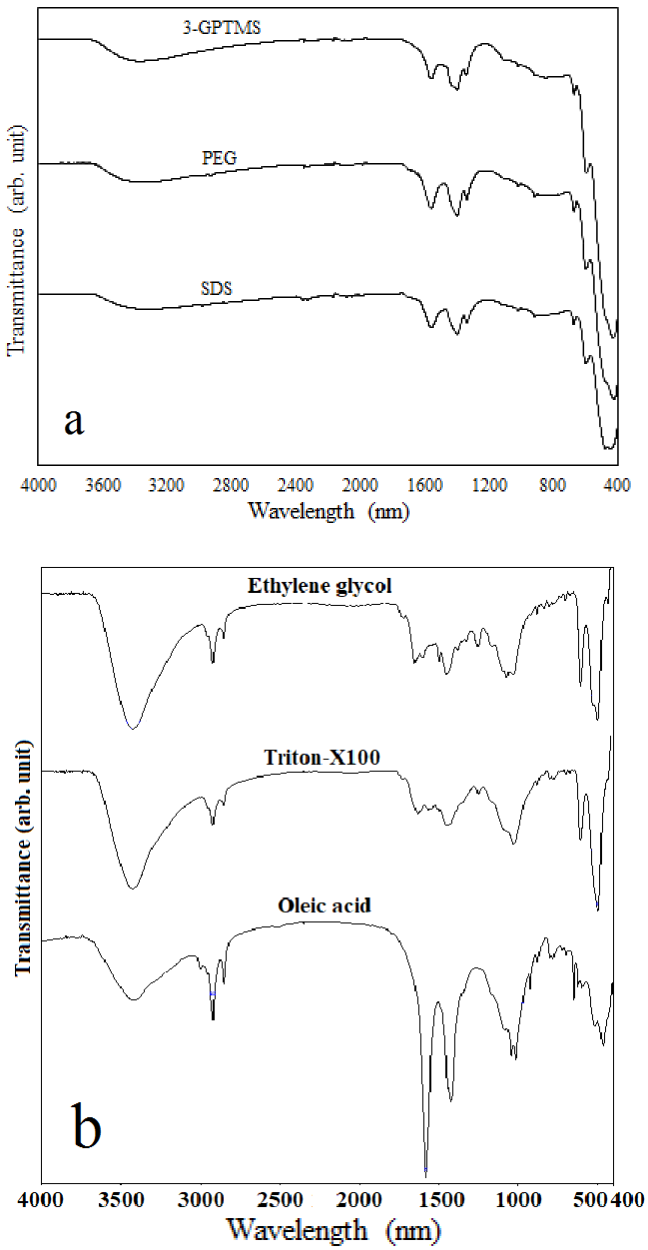

Figure 2: FTIR Spectra of CuO nano articles synthesized in the presence of a) SDS, PEG, 3-GPTMS and b) EG, Triton-100, Oleic acid.

SEM micrographs of CuO nano particles synthesized using of SDS, PEG, 3-GPTMS, EG, Triton-X100 and Oleic acid are shown in Figure 3a to f, respectively. As illustrated, all samples were composed mainly from highly agglomerated semi-spherical nano particles. For more appropriate microstructure study TEM technique was used. TEM micrographs of samples using of SDS, PEG, 3-GPTMS and EG are shown in Figure 4a to d, respectively. As shown in Figures 4a,b and d, nano particles synthesized in the presence of SDS, PEG and EG were less than 15 nm in

size, and were agglomerated irregularly. However, synthesis in the presence of 3-GPTMS led to formation of larger (>30 nm) semispherical nano particles, which may be attributed to the dual role of surface modification and stabilization, or could also be related to the activation of the Ostwald ripening mechanism. Piri et al. [28] and Khosravi et al. [38] in two distinct researches show that some SMs play a significant role in particle morphology. For example, using PVP and CTAB caused to formation of oriented microstructures such as rods. Nevertheless, the common feature of all the SMs used in the present study is that the particle morphology is mostly irregular and tends toward spherical, with a high degree of agglomeration. This tendency arises from the fine-grained nature of the particles. Simultaneous evaluation of SEM and TEM micrographs reveals that the particles exhibit quantum dot behavior and are below the quantum confinement limit [28]. However, a clear difference in the degree of agglomeration was observed, indicating the varying ability of the SMs to cover the particle surfaces. Primarily van der Waals attractions and incomplete surface passivation during precipitation, leading to oriented attachment or soft agglomeration. Surface modifiers reduce this via steric/electrostatic stabilization; e.g., SDS and Oleic Acid provide better repulsion than others [36, 39].

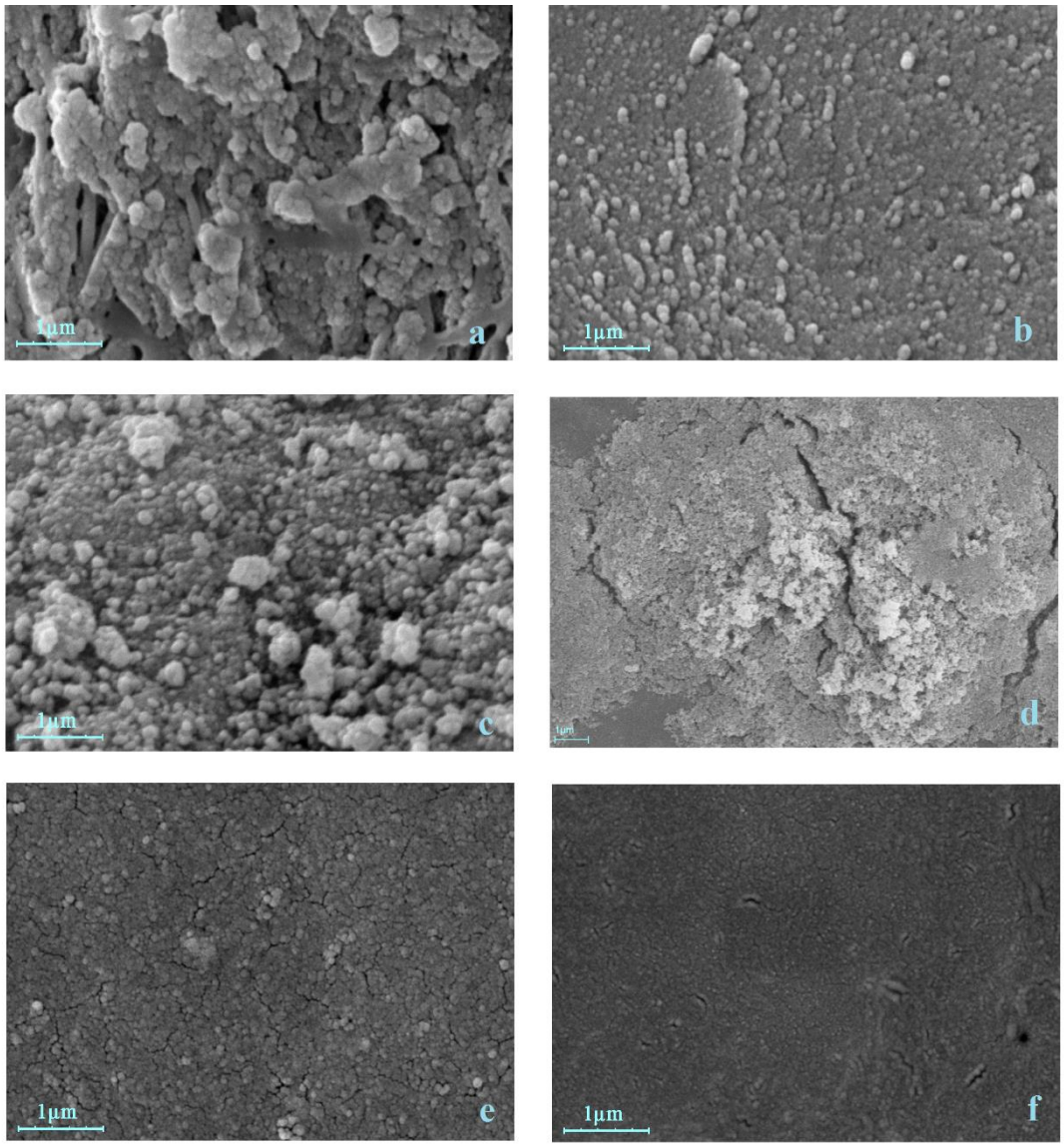

Figure 3: SEM micrographs of CuO nano particles synthesized in the presence of a) SDS, b) PEG, c) 3-GPTMS, d) EG, e) Tiron-100 and f) Oleic acid.

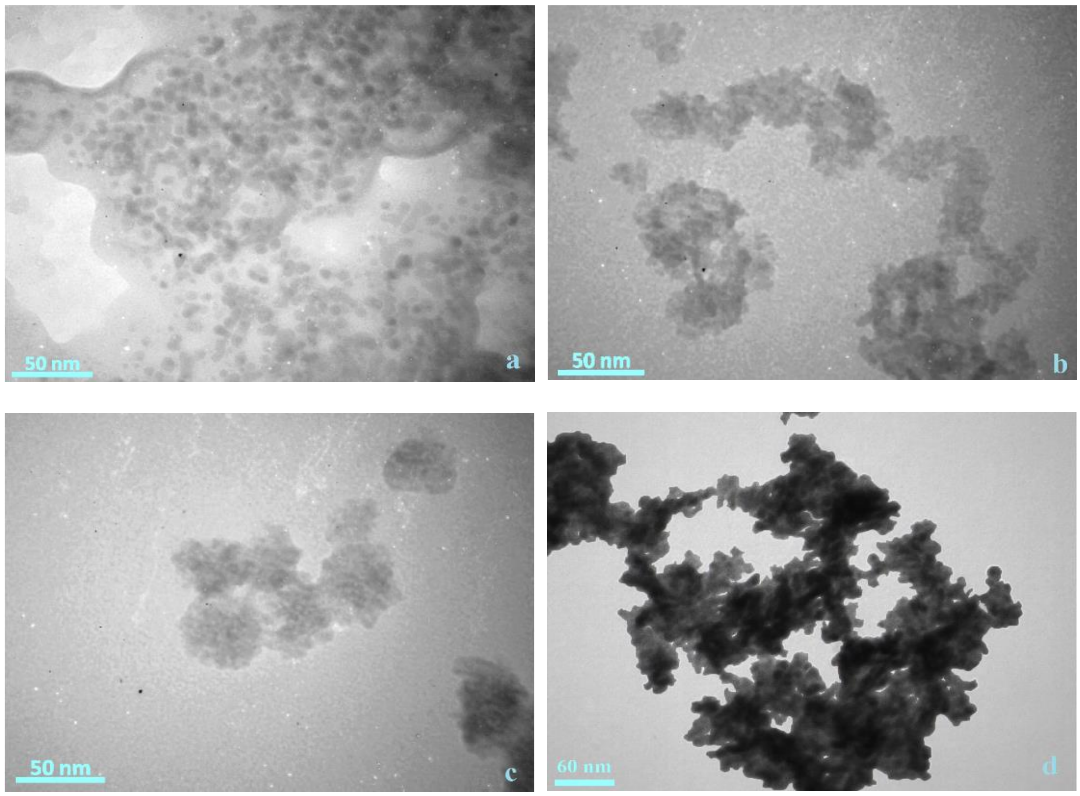

Figure 4: TEM micrographs of CuO samples nano particles synthesized in the presence of a) SDS, b) PEG, c) 3-GPTMS and d) EG.

TEM micrographs also clearly show that SDS leads to the formation of CuO particles with higher dispersibility. The irregular, nearly spherical shape of the particles suggests that the growth mechanism of the primary particles follows diffusion-controlled growth, whereby the particles do not retain their initial structural shape and become spherical.

Figure 5a shows UV-Visible spectra of powders synthesized using various SMs. The broad absorption peak is related to the surface plasmon resonance (SPR) [40], where changes in the shape and location of the peaks depend on the shape, size, and size distribution of the particles. Broadening in some spectral ranges and sharpness in others arise from the wide size distribution of the particles. The absorption peaks below 300 nm correspond to interband transitions from deep levels of copper atoms and their oxides. The absorption peaks between 300 and 400 nm are related to copper oxide nanoparticles and result from charge transfer from oxygen to copper ions [41]. Furthermore, the peaks above 400 nm are attributed to the green color nature of copper oxide [42]. Using the spectra Data and Tauc equation, curves of $(\alpha h\nu)^2$ as a function of $h\nu$ were plotted (Figure 5b) and band gaps of CuO nano particles were calculated and given in Table 1. According to Table 1 and Figure 5b, the calculated band gap values for all samples synthesized using various SMs are more than that of bulk CuO (1.2 eV), which is associated to the quantum confinement effect. When the particle size is about the de Broglie wavelength of charge carriers, the band gap value increases due to the particle size effect and the quantization of energy levels [43]. Such increase of band gap values using SMs were reported by some researchers [28, 29] and Bandgap values as high as 4 eV have been reported, indicating extremely small particle sizes and placement within the quantum dot region [36]. In addition, an inverse relationship between crystallite size and band gap is observed. As expected, the presence of SDS led to the smallest size and crystallite size, and consequently the most band gap value. In contrast, the 3-GPTMS resulted in the largest particles (Figure 3c) and the least band gap value i.e. 2.6 eV. Although the overall crystalline phases (monoclinic CuO) and average particle sizes remained largely consistent across samples, the observed band gap values (ranging from 2.6 eV with 3-GPTMS to 4.02 eV with SDS) can be attributed to subtle differences in

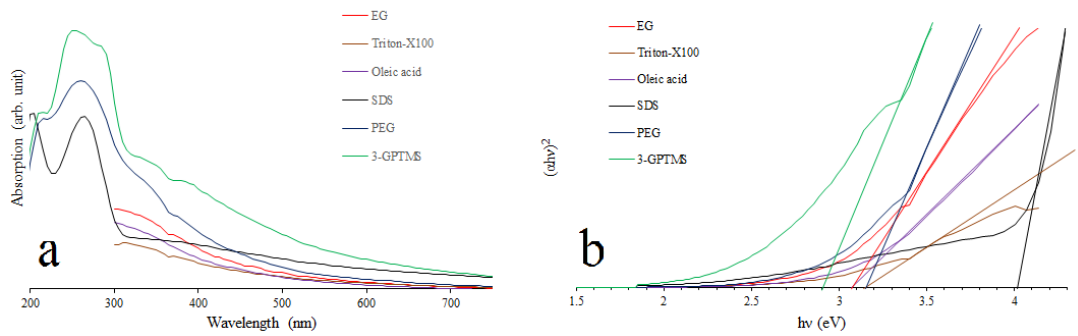

Figure 5: a) UV spectra and b) $(\alpha hv)^2$ versus hv of CuO nano particles synthesized in the presence of various SMs.

Table 1: Band gaps of CuO nanoparticles synthesized in the presence of different SMs.

Surface Modifier	SDS	PEG	3-GPTMS	EG	Triton-X100	Oleic acid
Band gap (eV)	4.02	3.15	2.6	3.1	3.15	3.1

surface chemistry, defect states, and localized quantum confinement effects induced by the different SMs. Surface modifiers interact variably with the nanoparticle surface, influencing surface passivation, oxygen vacancies, or micro-strain, which modulate the electronic structure [28, 44]. For instance, SDS (anionic) may promote stronger surface capping and higher defect density leading to significant blue-shift (4.02 eV), while 3-GPTMS (silane-based) allows different bonding that results in less widening (2.6 eV). These variations align with reports on surfactant-mediated synthesis of CuO, where band gap widening occurs even with minor size differences due to quantum confinement and surface effects [28].

4. Conclusions

The present work copper oxide nanoparticles were synthesized using SDS, PEG, 3-GPTMS, EG, Triton-X100 and Oleic acid SDs. XRD patterns confirmed that nano copper oxide particles with no minor phase and crystallite size of 6-10 nm were obtained. FTIR spectra showed the characteristic Cu-O bond bands in all samples. SEM Micrographs revealed that all samples consisted of highly agglomerated, semispherical nano-particles. Furthermore, transmission electron micros-copy (TEM) confirmed that synthesized powders were in nano scale range. Moreover, synthesis in the presence of SDS led to the smallest nanoparticles, while the use of 3-GPTMS resulted in the largest. The notable broadening of the band gap values up to 4eV in the powders further supports the great band splitting and nanoscale nature of the synthesized particles, in comparison with bulk CuO (1.2eV).

5. References

1. Amrut. S. Lanje, Satish J. Sharma, Ramchandara B. Pode, Raghumani S. Ningthoujam. Synthesis and optical characterization of copper oxide nanoparticles, Adv.Appl. Sci. Res. 2010; 1(2):36-40.
2. Zhang M, Lv X, Wang T, Pei W, Yang Y, Li F et al. CuO-based gas sensor decorated by polyoxometalates electron acceptors: From constructing heterostructure to improved sensitivity and fast response for ethanol detection, Sensors Actuators B: Chem. 2024; 415: 136016. https://doi.org/10.1016/j.snb.2024.136016.
3. Steinhauer S. Gas Sensors based on copper oxide nanomaterials: a review, Chemosensors. 2021;9(3):51. https://doi.org/10.3390/chemosensors9030051.
4. Bhat N, Ukkund SJ, Ashraf M, Acharya K, J Ramegouda N, Puthiyillam P. et al. GO/CuO nanohybrid-based carbon dioxide gas sensors with an

arduino detection unit, ACS Omega. 2023; 8(36): 32512-9. https://doi.org/10.1021/acsomega.3c02598.
5. Nahar B, Chaity SB, Gafur MA, Hossain MZ. Synthesis of spherical copper oxide nanoparticles by chemical precipitation method and investigation of their photocatalytic and antibacterial activities, J Nanomater. 2023; 2023:1-10. https://doi.org/10.1155/2023/ 2892081.
6. Benaissa N, Garmim T, El Boughdadi M, El Jouad Z, Louardi A, Hartiti B et al. Experimental and numerical simulation studies of CuO thin films based solar cells. Eng Res Express. 2023; 5(4):45038. https://doi.org/10.1088/2631-8695/ad05b3.
7. Akter S, Sikdar TT, Sultana M, Ahmed S, Bashar MS, Rahman MK. Enhancing the performance of CuO thin film in solar cell by introducing optimum amount of Ni doping, J Mater Sci: Mater Electron. 2024;35 (19): 1299. https://doi.org/10.1007/s10854-024-13053-x.
8. Singh J, Lee S, Tomar A, Zulkifli, Kim J, Kumar Rai A. Surfactant-mediated synthesis of novel mesoporous hollow CuO nanotubes as an anode material for lithium-ion battery application. ChemistrySelect. 2023;8(1). https://doi.org/10.1002/slct.202203755.
9. Sibhatu AK, Weldegebrieal GK, Sagadevan S, Tran NN, Hessel V. Photocatalytic activity of CuO nanoparticles for organic and inorganic pollutants removal in wastewater remediation, Chemosphere. 2022;300:134623.https://doi.org/10.1016/j.chemosphere.2022.134623.
10. Raizada P, Sudhaik A, Patial S, Hasija V, Parwaz Khan AA, Singh P et al. Engineering nanostructures of CuO-based photocatalysts for water treatment: Current progress and future challenges. Arabian J Chem. 2020;13(11):8424-57. https://doi.org/10.1016/j.arabjc.2020.06.031.
11. Lakshmanan A, Alex ZC, Meher SR. Recent advances in cuprous oxide thin film based photovoltaics. Mater Today Sustain. 2022; 20:100244. https://doi.org/10.1016/j.mtsust.2022.100244.
12. Amin HIM, Hamadamin AH, Issa KD, Shareef SH, Abdullah VS, Othman HO. et al. Synthesis of copper oxide nanoparticles from Ixiolirion tataricum: Assessment of their antimicrobial, antioxidant, and enzyme inhibitory activity. Inorg Chem Commun. 2026; 184: 116024. https://doi.org/10.1016/j.inoche.2025.116024.
13. Phiwdang K, Suphankij S, Mekprasart W, Pecharapa W. Synthesis of CuO nanoparticles by precipitation method using different precursors, Energy Procedia. 2013;34:740-5. https://doi.org/10.1016/j.egypro. 2013.06.808
14. Sahooli M, Sabbaghi S, Saboori R. Synthesis and characterization of mono sized CuO nanoparticles. Mater Lett. 2012;81:169-72. https://doi.org/10.1016/j.matlet.2012.04.148
15. Rahimi-Nasrabadi M, Pourmortazavi SM, Davoudi-Dehaghani AA, Hajimirsadeghi SS, Zahedi MM. Synthesis and characterization of copper oxalate and copper oxide nanoparticles by statistically optimized controlled precipitation and calcination of precursor, Cryst Eng Comm. 2013;15(20):4077-86. https://doi.org/ 10.1039/C3CE26930B.
16. Rahnama A, Gharagozlou M. Preparation and properties of semiconductor CuO nanoparticles via a simple precipitation method at different reaction temperatures. Opt Quant Electron. 2012; 44(6-7):313-22. https://doi.org/10.1007/s11082-011-9540-1.
17. John AS, Gurumurthy K. Synthesis and characterization of CuO nanoparticles from bioleached copper through modified and optimized double precipitation method, ACS Omega. 2025;10(10):10193-8. https://doi.org/10.1021/acsomega.4c09064.
18. Sabbaghan M, Beheshtian J, Niazmand Liarjdame R. Preparation of Cu_2O nanostructures by changing reducing agent and their optical properties. Mater Lett. 2015; 153:1-4. https://doi.org/10.1016/j.matlet.2015.03.147.
19. Khaled IM, Umair M, Pecoraro CM, Kheniche A, Bellardita M, Soltani S. Green synthesis of ZnO and CuO nanoparticles and ZnO-CuO nanocomposites: Characterization and photocatalytic dyes removal efficiency's determination, Colloids Surf A: Physicochem Eng Aspect. 2026; 728:138544. https://doi.org/10.1016/j.colsurfa.2025.138544.
20. Mandal S, Hazra C, Joshi N, Kumar P, Sen R, Das S et al. Comparative insights of bio and chemical surfactants in CuO nanoparticle synthesis: Unveiling the superior antibacterial efficacy of biosurfactants, J Indust Eng Chem. 2025; 147:566-83. https://doi.org/10.1016/j.jiec.2024.12.046.
21. Siddiqui H, Qureshi MS, Haque FZ. Surfactant assisted wet chemical synthesis of copper oxide (CuO) nanostructures and their spectroscopic analysis, Optik. 2016; 127(5):2740-7. https://doi.org/10.1016/j.ijleo.2015.11.220.
22. Ravishankar TN, Vaz MdO, Teixeira SR. The effects of surfactant in the sol–gel synthesis of CuO/TiO_2 nanocomposites on its photocatalytic activities under UV-visible and visible light illuminations, New J Chem. 2020; 44(5):1888-904. https://doi.org/10.1039/C9NJ05246A.
23. Abdel-Monem YK, Emam SM, Okda HMY. Solid state thermal decomposition synthesis of CuO nanoparticles from coordinated pyrazolopyridine as novel precursors, J Mater Sci Mater Electron. 2017; 28(3):2923-34. https://doi.org/10.1007/s10854-016-5877-3.
24. Abdelghany MM, Ahmed IS, Dessouki HA, Abdelrahman EA. Facile synthesis of CuO and Ag nanoparticles by thermal decomposition of novel schiff base complexes, J Inorg Organomet Polym. 2021;31(11):4281-99. https://doi.org/10.1007/s10904-021-02032-y.
25. Singh Z, Singh I. CTAB surfactant assisted and high pH nano-formulations of CuO nanoparticles pose greater cytotoxic and genotoxic effects, Sci Rep. 2019; 9(1):5880. https://doi.org/10.1038/s41598-019-42419-z.

26. Silva N, Ramírez S, Díaz I, Garcia A, Hassan N. Easy, Quick, and reproducible sonochemical synthesis of CuO nanoparticles, Materials (Basel). 2019; 12(5). https://doi.org/10.3390/ma12050804.
27. Vaseem M, Hong AR, Kim R-T, Hahn YB. Copper oxide quantum dot ink for inkjet-driven digitally controlled high mobility field effect transistors, J Mater Chem C. 2013;1(11):2112. https://doi.org/10.1039/c3tc00869j.
28. Piri F, Shafiee Afarani M, Arabi AM. Synthesis of copper oxide quantum dots: effect of surface modifiers, Mater Res Express. 2019; 6(12):125006. https://doi.org/10.1088/2053-1591/ab548d.
29. Shafiee Afarani M, Safaei L. Synthesis of copper oxide nano particles: Effect of rosemary and olive leaf extracts as surface modifier, CNMST. 2026; 2(13):57-62. https://doi.org/10.22111/cnmst.2026.54636.1280.
30. Sallem F, Chanéac C, Wagner M, Rataj N, Annabi E, Castillo A et al. Controlled synthesis of copper oxide nanoparticles (CuONPs) by the precipitation method and proposition of their growth mechanism, Nanoscale. 2026; 18(10):5436-46. https://doi.org/ 10.1039/d5nr04826e.
31. Abbasian AR, Shafiee Afarani M. One-step solution combustion synthesis and characterization of $ZnFe_2O_4$ and $ZnFe1.6O_4$ nanoparticles, Appl Phys A. 2019; 125(10). https://doi.org/10.1007/s00339-019-3017-7
32. Zhao J, Yang G, Zhang Y, Zhang S, Zhang C, Gao C et al. Controllable synthesis of different morphologies of CuO nanostructures for tribological evaluation as water-based lubricant additives, Friction. 2021;9(5): 963-77. https://doi.org/10.1007/s40544-020-0382-3.
33. Soleimani E, Taheri R. Synthesis and surface modification of CuO nanoparticles: Evaluation of dispersion and lipophilic properties, Nano-Struct Nano-Object. 2017;10:167-75. https://doi.org/10.1016/j.nanoso.2017.05.002.
34. Troudi B, Halimi O, Sebais M, Boudine B, Djebli A. Synthesis, Structural and optical properties of CUO nanocrystals embedded in polyvinyl chloride (PVC) thin films, Inter J Mechan Product Eng (IJMPE). 2017; 5(2):115-9.
35. Angeline Mary AP, Thaminum Ansari A, Subramanian R. Sugarcane juice mediated synthesis of copper oxide nanoparticles, characterization and their antibacterial activity. J King Saud University Sci. 2019; 31(4):1103-14. https://doi.org/10.1016/j.jksus. 2019. 03.003.
36. Ramzan I, Khan BS, Hayat SS, Hyder S, Asmat N, Shakir B et al. SDS stabilized CuO nanoparticles as dual functional agents for antifungal and photo-catalytic applications, Discover Sustain. 2025; 6(1): 703. https://doi.org/10.1007/s43621-025-01654-3.
37. Afsharimani N, Durán A, Galusek D, Castro Y. Hybrid sol–gel silica coatings containing graphene nanosheets for improving the corrosion protection of AA2024-T3, Nanomaterials. 2020;10(6):1050. https://doi. org/10.3390/nano10061050.
38. Khosravi MD, Ghahari M, Shafiee Afarani M, Arabi AM. Synthesis of CuO and CuO/ZnO composite powders for antibacterial, photocatalytic, and pigment-related applications, Adv Ceram Prog. 2022; 8(1):1-8. https://doi.org/10.30501/acp.2022.329820.1082.
39. Almeida JC de, Rodrigues TA, Da Silva GTST, Ribeiro C, Mendonça VR de. Unveiling the influence of alkaline modifiers in CuO synthesis on its photocatalytic activity for CO_2 reduction, Mater Adv. 2024;5(16):6479-88. https://doi.org/10.1039/D4MA00337C.
40. Singh G, Panday S, Rawat M, Kukkar D, Basu S. Facile Synthesis of CuO semiconductor nanorods for time dependent study of dye degradation and bioremediation applications. J Nano Res. 2017; 46:154-64. https://doi.org/10.4028/www.scientific.net/JNanoR.46.154.
41. Rawat R, Tiwari A, Arun N, Rao, S. V. S. Nageswara, Pathak AP, Rao SV et al. Synthesis of CuO hollow nanoparticles using laser ablation: effect of fluence and solvents. Appl Phys A. 2020; 126 (3):226. https://doi.org/10.1007/s00339-020-3403-1.
42. Keabadile OP, Aremu AO, Elugoke SE, Fayemi OE. Green and traditional synthesis of copper oxide nano-particles-comparative study, Nanomaterials. 2020;10 (12):2502. https://doi.org/10.3390/nano10122502.
43. Wang H, Xu J-Z, Zhu J-J, Chen H-Y. Preparation of CuO nanoparticles by microwave irradiation, J Crystal Growth. 2002;244(1):88-94. https://doi.org/10.1039/C6RA13876D.
44. Maria KH, Rodriguez Bonet SG, Bosco MV, Bin Salam SR, Dhar D, Nazzarro M et al. Synthesis and characterization of CuO nanoparticles using heat treatment approach: annealing effects on crystallite size and band Gap of CuO nanoparticles, ACS Omega. 2026;11(7):11141-54. https://doi.org/10.1021/acsomega.5c06800.

How to cite this article:
Shafiee Afarani M, Arabi AM, Kordi-Tamandani H, Ramezani F, Kaykhaii M. Synthesis of Copper Oxide Nano Powders: Effect of Surface Modifier Type. Prog Color Colorants Coat. 2027;20(2): 193-201. https://doi.org/10.30509/pccc.2026.167790.1501.